

CALCULATION OF FINNED TUBE PRESSURE DROP AND HEAT TRANSFER USING FULLY THREE-DIMENSIONAL CFD METHODS

Christopher J. Matice, P.E.
Brian Gao
Stress Engineering Services, Inc.

Abstract

The use of computational fluid dynamics (CFD) in the design and troubleshooting of HRSGs is now well established. However, the large ratio of scales between the overall flow path and the tube bundles themselves means that the bundles must be approximated using “porous media” models, with heat transfer and flow resistance simulated using lumped parameters. The parameters input into these models are taken from the open literature, proprietary data, and/or approximate analytical models. In the case of plain tubes, two-dimensional CFD models have been used to supplement this information. For the finned tubes used in HRSGs, however, 2D models will not suffice and 3D models can quickly become unwieldy. In this work we present the results of a parametric study of pressure drop and heat transfer for finned tube bundles computed using fully three-dimensional CFD models. The results are compared with values computed from correlation equations typically used in design. The advantages and limitations of this approach to obtaining inputs for HRSG tube bundle simulations are discussed.

Introduction

This work was motivated by a desire to use computational methods to predict the onset of flow-induced vibration (FIV) in the leading superheater tube bundles of heat recovery steam generators (HRSG). These bundles are susceptible to vibration caused by turbulent buffeting as the flow from the gas turbine impinges upon the leading tubes and, to a lesser extent, familiar FIV mechanisms such as fluid-elastic whirl and vortex shedding. In the case of plain tubes experiencing uniform flow, two-dimensional coupled flow and stiffness models, such as that shown in Figure 1 have been used to successfully simulate FIV. In the case of a HRSG, however, the tubes are typically finned and the approach velocity is far from uniform. Even if we simplify the problem, considering a span over which the approach velocity can be considered to be approximately uniform, we are still left with the problem of modeling the fins. This requires a three-dimensional flow model.

As a first step in the development of a 3D FIV model, the flow portion of the problem is addressed in isolation. The goal is to determine how well a reasonably-sized computational fluid dynamics (CFD) model could predict the flow versus pressure relationship for a representative finned tube bundle. Comparisons of the CFD results with correlation equations for flow loss in

bundles are used to evaluate the performance of the CFD model. Numerical and turbulence modeling issues are also addressed.

While the desire to perform fully 3D FIV simulations motivates this work, the flow model alone is of value in predicting the steady-state performance of a bundle. This is particularly the case for typical HRSG bundles that includes tubes of varying diameter and fins of varying height and pitch within a single bundle. Therefore, thermal calculations are performed using the CFD models and compared with correlation equations commonly used in the industry.

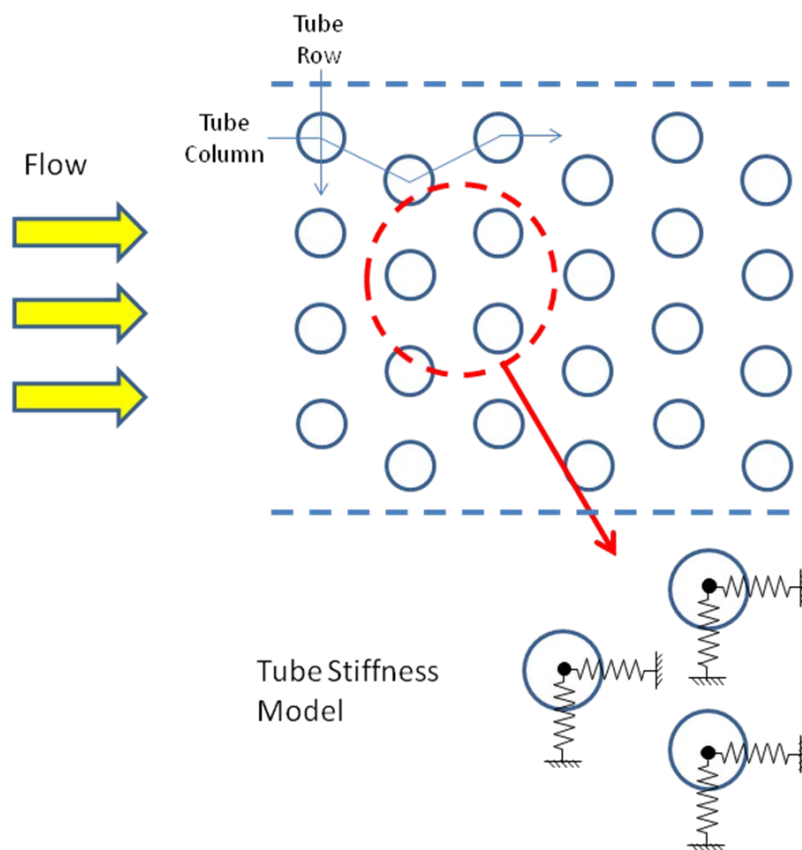


Figure 1
Two-dimensional Flow-Induced Vibration Model of Tube Bundle

Model Setup and Parameter Study Definition

The layout of the tube bundle analyzed is shown in Figure 2. Typical HRSG superheater bundles range from 3 to 8 tube rows in depth; a six-row bundle is chosen for this analysis. The values of several important parameters are varied, producing a set of eleven cases, as shown in Table 1.

These parameters are:

| | |
|-----------------------------|-------------------|
| V_{approach} | Approach velocity |
| d | Tube diameter |
| P | Tube pitch |
| h_{fin} | Fin height |
| p_{fin} | Fin pitch |
| t_{fin} | Fin thickness |

These parameters are non-dimensionalized, as shown in Table 2, with the Reynolds number defined as

$$\text{Re} = \frac{V_{\text{approach}} d}{\nu}, \quad (1)$$

where ν is the kinematic viscosity of air at the approach temperature.

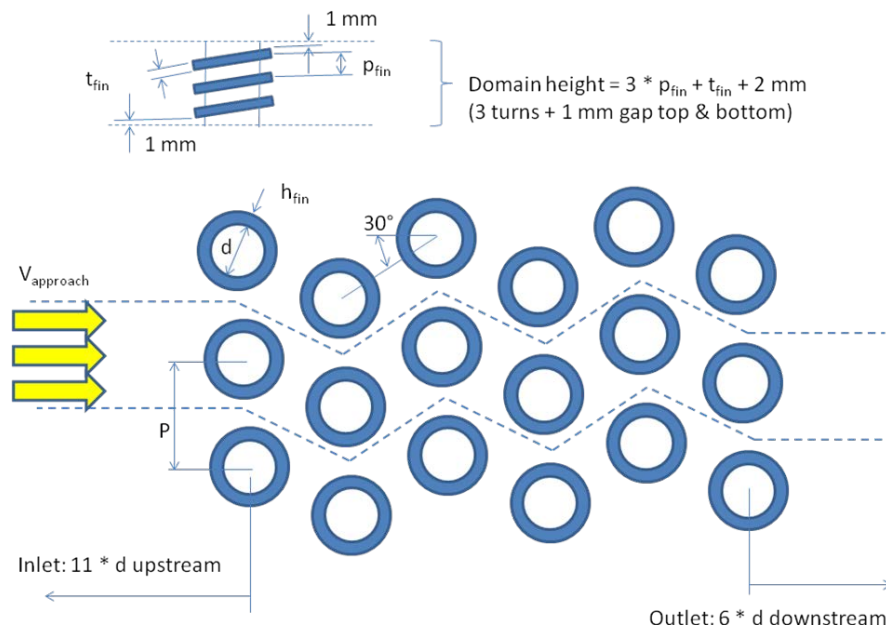


Figure 2
Model Definition

Table 1
Parameter List - Dimensional

| Case | V_{approach} | d | P | h_{fin} | p_{fin} | t_{fin} |
|------|-----------------------|------|------|------------------|------------------|------------------|
| | (m/s) | (mm) | (mm) | (mm) | (mm) | (mm) |
| 1 | 15 | 40 | 100 | 10 | 5 | 1 |
| 2 | 7.5 | 40 | 100 | 10 | 5 | 1 |
| 3 | 30 | 40 | 100 | 10 | 5 | 1 |
| 4 | 15 | 40 | 80 | 10 | 5 | 1 |
| 5 | 15 | 40 | 120 | 10 | 5 | 1 |
| 6 | 15 | 40 | 100 | 8 | 5 | 1 |
| 7 | 15 | 40 | 100 | 12 | 5 | 1 |
| 8 | 15 | 40 | 100 | 10 | 4 | 0.8 |
| 9 | 15 | 40 | 100 | 10 | 6 | 1.2 |
| 10 | 15 | 40 | 100 | 10 | 5 | 0.8 |
| 11 | 15 | 40 | 100 | 10 | 5 | 1.2 |

Table 2
Parameter List – Non-Dimensional

| Case | Re | P/d | h_{fin}/d | p_{fin}/d | $t_{\text{fin}}/p_{\text{fin}}$ |
|------|-------|-----|--------------------|--------------------|---------------------------------|
| 1 | 7264 | 2.5 | 0.25 | 0.125 | 0.2 |
| 2 | 3632 | 2.5 | 0.25 | 0.125 | 0.2 |
| 3 | 14528 | 2.5 | 0.25 | 0.125 | 0.2 |
| 4 | 7264 | 2 | 0.25 | 0.125 | 0.2 |
| 5 | 7264 | 3 | 0.25 | 0.125 | 0.2 |
| 6 | 7264 | 2.5 | 0.2 | 0.125 | 0.2 |
| 7 | 7264 | 2.5 | 0.3 | 0.125 | 0.2 |
| 8 | 7264 | 2.5 | 0.25 | 0.1 | 0.2 |
| 9 | 7264 | 2.5 | 0.25 | 0.15 | 0.2 |
| 10 | 7264 | 2.5 | 0.25 | 0.125 | 0.16 |
| 11 | 7264 | 2.5 | 0.25 | 0.125 | 0.24 |

The symmetry of the bundle is exploited by modeling only one column of tubes, as shown by the dashed lines in Figure 2. The surfaces represented by these lines must be treated as periodic boundaries, wherein flow leaving from one boundary reenters on the opposite boundary. The CFD model constructed from Figure 2 is shown in Figure 3. The model mesh is shown in Figure 4. This mesh is based on the smallest length scale in the problem, the fin thickness, resulting in an element size of approximately 1 mm and giving approximately one element for every 3 degrees of arc around each tube (126 elements around each tube). The total number of elements is approximately 2 million.

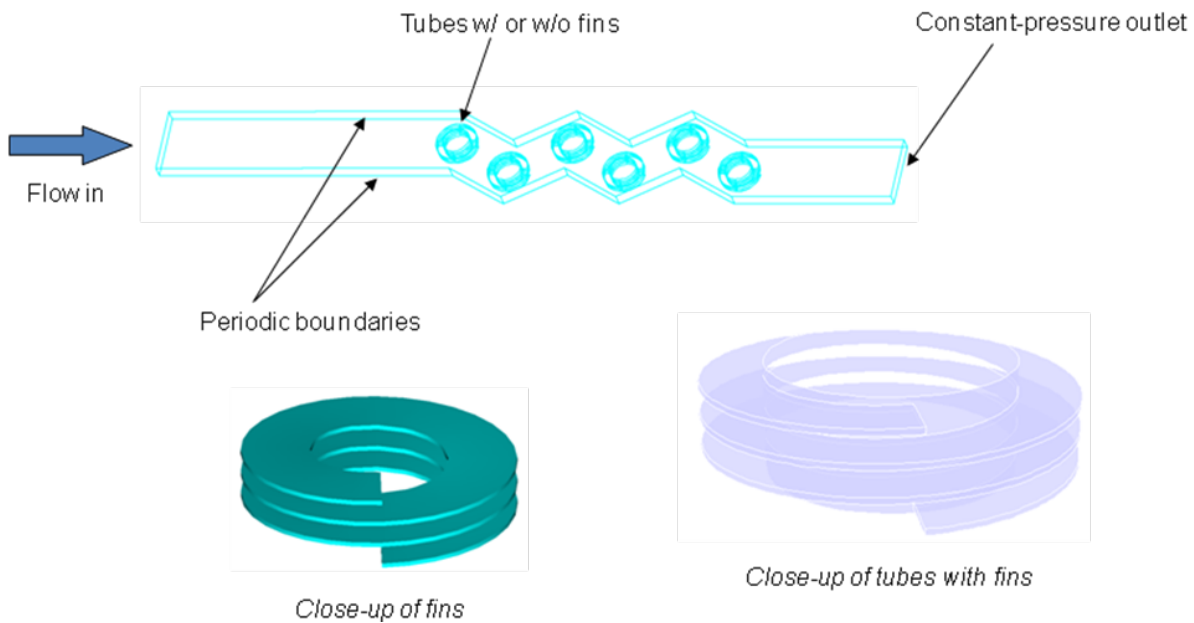


Figure 3
Model Layout

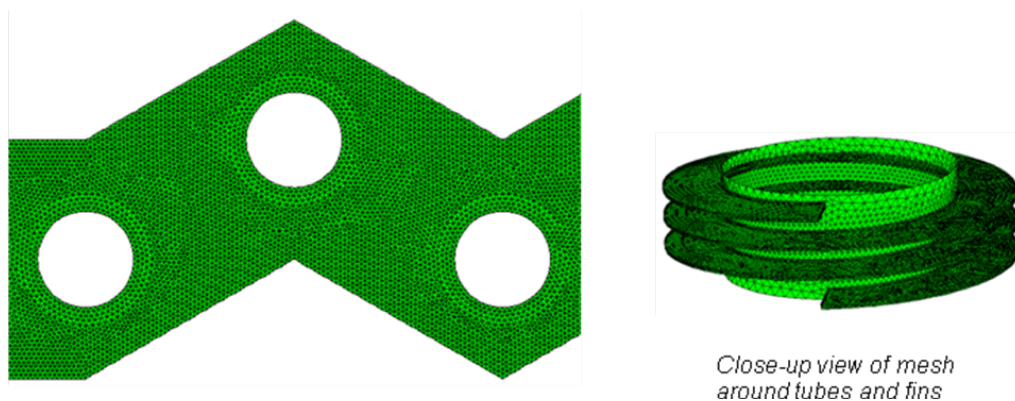


Figure 4
Typical Mesh

The periodic symmetry imposed on the CFD model allows for sufficient detail to simulate steady-state flow and heat transfer in the tube bundle. However, simulation of unsteady behavior leading to FIV would require that multiple columns of tubes be modeled. The absolute minimum number of columns modeled should be six. This allows two columns of rigid tubes to form the boundaries of the model and four columns of mobile tubes. In the current case this would result in a model of 12 million elements. Therefore, even a very restricted model will be quite large.

The model is analyzed using the commercial CFD program FLUENT [1]. Material parameters for air at 800 °K (980 °F) are:

$$\begin{aligned}\rho &= 0.4413 \text{ kg/m}^3 \\ \nu &= 8.26\text{e-}5 \text{ m}^2/\text{s} \\ c_p &= 1099 \text{ J/kg-}^\circ\text{K} \\ k &= 0.0569 \text{ W/m-}^\circ\text{K}\end{aligned}$$

The fins are modeled using a conjugate heat transfer model and are assigned properties for steel as:

$$\begin{aligned}\rho &= 7800 \text{ kg/m}^3 \\ c_p &= 465 \text{ J/kg-}^\circ\text{K} \\ k &= 40 \text{ W/m-}^\circ\text{K}\end{aligned}$$

The tubes themselves are assigned a uniform temperature of 750 °K (890 °F). Simulations are performed for both finned and plain versions of each configuration. The plain-tube version is obtained by changing the fin material from steel to air. Therefore, the mesh is unchanged between the finned and plain versions of each configuration.

All solutions are performed using the k- ϵ turbulence model with FLUENT's enhanced wall functions (see below for discussion). Second-order interpolation is used for the momentum equations and a coupled solver is used to perform the iterative solution. Typical run times are on the order of 10 hours using one processor on a quad-core PC. Significant speed-up could be obtained through parallel processing. This would be necessary in analyzing a multi-column bundle model of a size sufficient to obtain FIV results (i.e. at least 6 columns of tubes).

Results

Color plots of results for Case 1 are shown in Figures 5 - 7. Some “wandering” of the wake is seen in many of the solutions, suggesting there may be a time-dependent component to the solution. A limited number of cases were rerun in transient mode. This showed a small variation in the solution with time but nothing appreciable. Therefore, all results presented herein are for steady-state conditions. The results in Figures 5 – 7 indicate that the upstream and downstream boundaries are adequately spaced to eliminate any influence of the boundary location on the solution. In fact, the inlet boundary could be moved significantly closer to the first tube, decreasing the mesh size by approximately 15%.

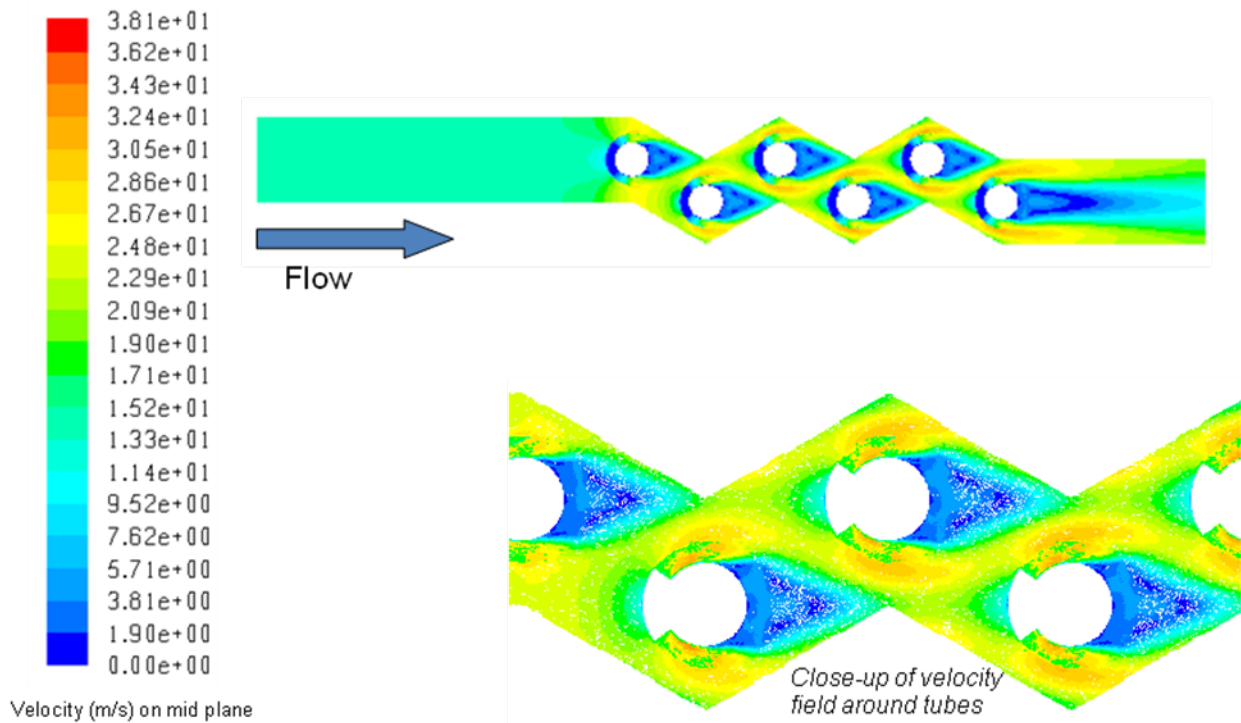


Figure 5
Velocity Results for Case 1

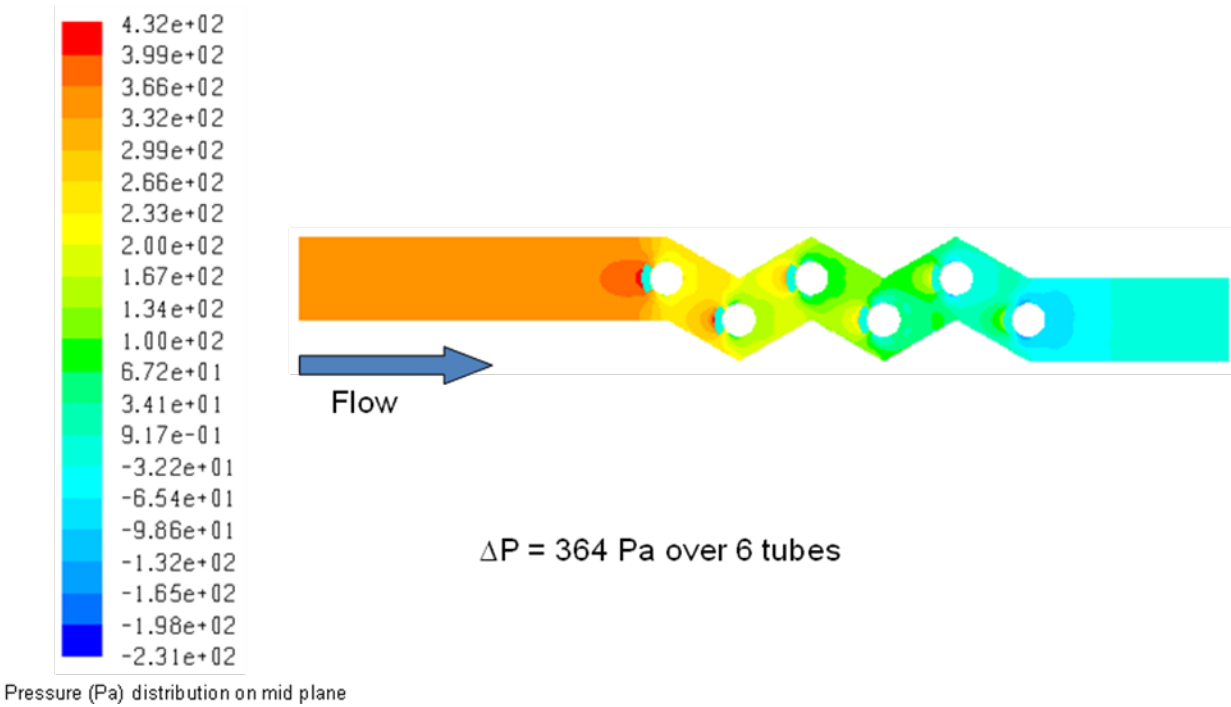


Figure 6
Pressure Distribution Results for Case 1

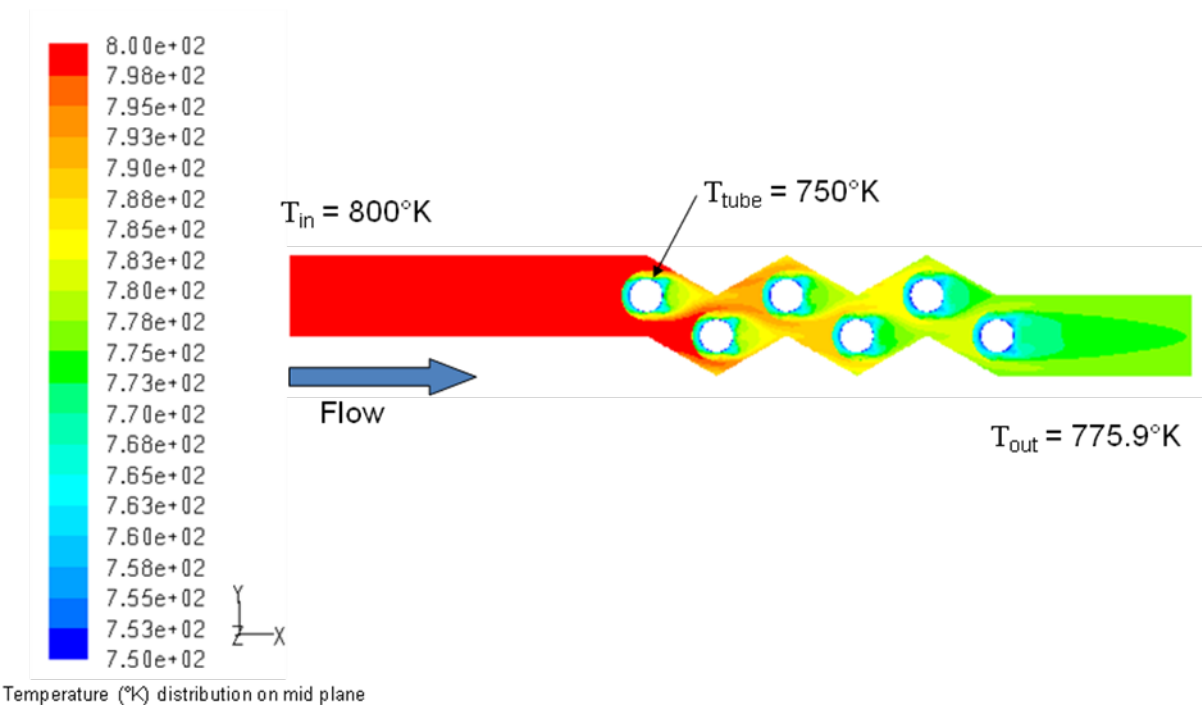


Figure 7
Heat Transfer Results for Case 1

The results of the parameter study are presented in Table 3. The pressure drop results are non-dimensionalized using the dynamic pressure in the gap between the tubes to obtain Euler numbers in the form given by Zukauskas and Ulinskas [2] as

$$Eu = \frac{\Delta p}{\frac{1}{2} \rho U^2 N}, \quad (2)$$

where N is the number of tubes in the bundle and U is the velocity in the gap between the tubes defined by

$$U = V_{\text{approach}} \frac{a}{a-1}, \quad (3)$$

with $a = P/d$.

Table 3
Parameter Study Results

| Case | Re | P/d | h_{fin}/d | p_{fin}/d | $t_{\text{fin}}/p_{\text{fin}}$ | Eu | | Nu | |
|------|-------|-----|--------------------|--------------------|---------------------------------|---------|----------|---------|----------|
| | | | | | | w/ fins | w/o fins | w/ fins | w/o fins |
| 1 | 7264 | 2.5 | 0.25 | 0.125 | 0.2 | 0.44 | 0.25 | 73.0 | 198 |
| 2 | 3632 | 2.5 | 0.25 | 0.125 | 0.2 | 0.60 | 0.31 | 53.3 | 139 |
| 3 | 14528 | 2.5 | 0.25 | 0.125 | 0.2 | 0.33 | 0.22 | 95.6 | 287 |
| 4 | 7264 | 2 | 0.25 | 0.125 | 0.2 | 0.52 | 0.29 | 83.2 | 216 |
| 5 | 7264 | 3 | 0.25 | 0.125 | 0.2 | 0.38 | 0.22 | 67.0 | 187 |
| 6 | 7264 | 2.5 | 0.2 | 0.125 | 0.2 | 0.40 | - | 80.3 | - |
| 7 | 7264 | 2.5 | 0.3 | 0.125 | 0.2 | 0.49 | - | 65.9 | - |
| 8 | 7264 | 2.5 | 0.25 | 0.1 | 0.2 | 0.47 | - | 64.6 | - |
| 9 | 7264 | 2.5 | 0.25 | 0.15 | 0.2 | 0.42 | - | 78.5 | - |
| 10 | 7264 | 2.5 | 0.25 | 0.125 | 0.16 | 0.42 | - | 69.2 | - |
| 11 | 7264 | 2.5 | 0.25 | 0.125 | 0.24 | 0.46 | - | 75.1 | - |

The change in temperature computed by the CFD model is used to compute the heat gain per meter of bundle length Q and the logarithmic mean temperature difference (LMTD) in the form

$$LMTD = \frac{T_{out} - T_{in}}{\ln[(T_{wall} - T_{in})/(T_{wall} - T_{out})]}, \quad (3)$$

where in all cases $T_{wall} = 750$ °K and $T_{in} = 800$ °K. The heat transfer coefficients are then computed as

$$\bar{h} = \frac{Q}{A_{total} LMTD}, \quad (4)$$

where A_{total} is the total surface area of the tubes and fins. The heat transfer coefficients are non-dimensionalized to obtain Nusselt numbers in the form:

$$Nu = \frac{\bar{h}L}{k}, \quad (5)$$

where, following Gnielinski, et al [3], $L = d$ for finned tubes and $L = \pi d/2$ for plain tubes.

The effect of each of the five parameters on both pressure drop and heat transfer is shown in Figures 8 – 12. The effects rank in order with the figure numbers, with Reynolds number having the greatest effect, followed by tube pitch and the fin parameters. Note that the effect of acceleration through the tube bundle is already accounted for by the use of the velocity in the narrowest gap to compute the dynamic pressure used to compute Eu . Therefore, the pitch effect shown in Figure 9 is independent of the effect of acceleration through the narrowest gap.

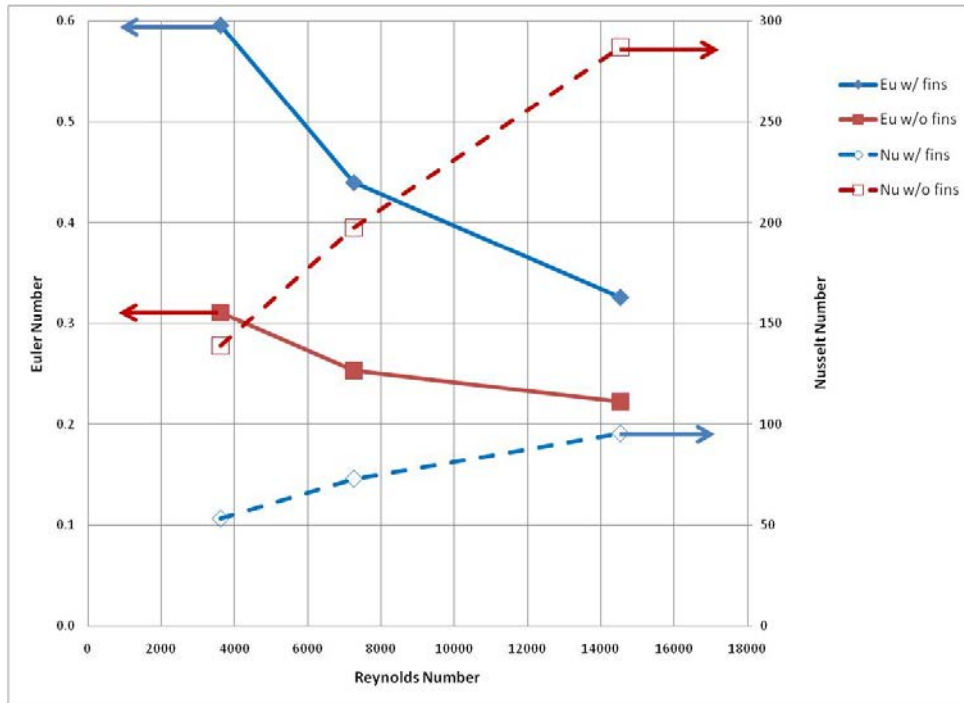


Figure 8
Dependence of Pressure Drop and Heat Transfer on Reynolds Number

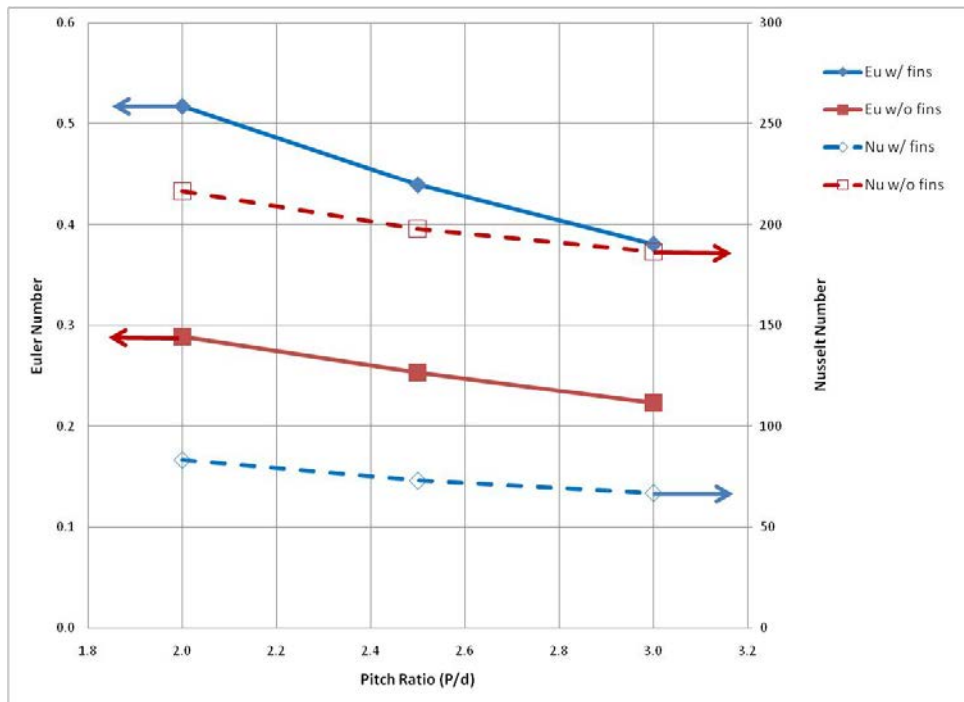


Figure 9
Dependence of Pressure Drop and Heat Transfer on Tube Pitch

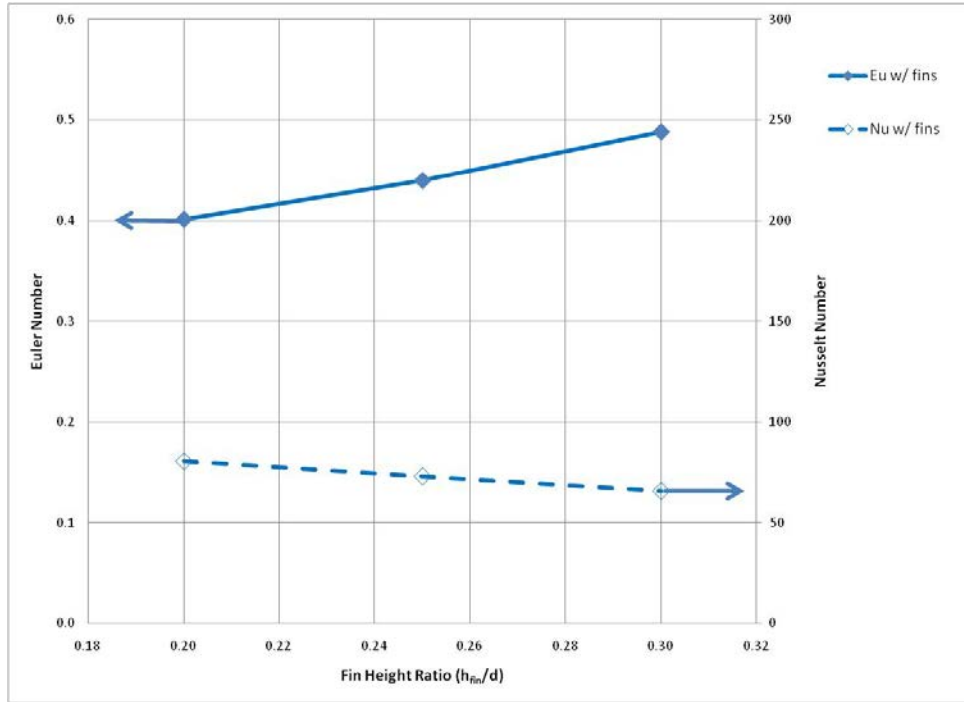


Figure 10
Dependence of Pressure Drop and Heat Transfer on Fin Height

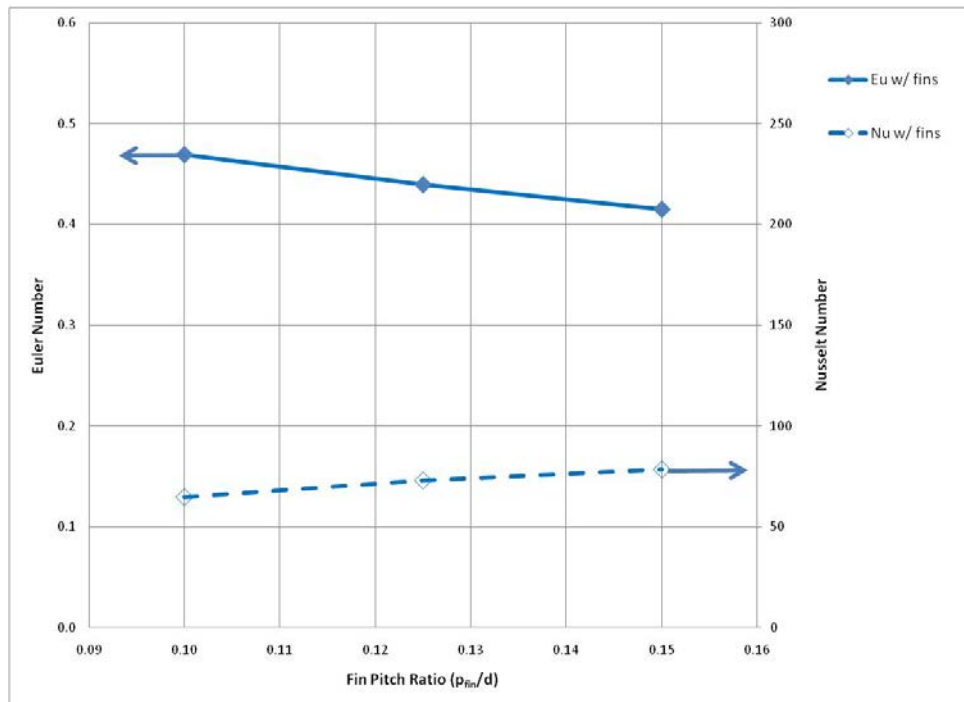


Figure 11
Dependence of Pressure Drop and Heat Transfer on Fin Pitch

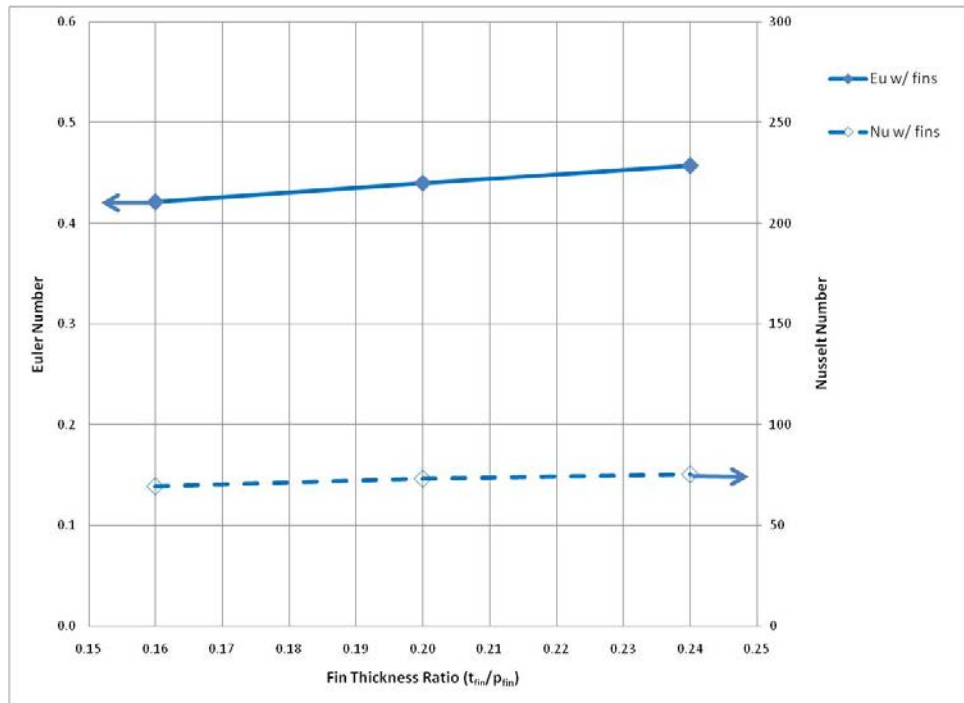


Figure 12
Dependence of Pressure Drop and Heat Transfer on Fin Thickness

Comparison with Correlation Equations

The CFD results are compared with values of Eu and Nu computed from correlation equations provided in references [2], [3], and [4]. The comparisons are presented in Table 4 as ratios of the values computed from the CFD models (see Table 3) to the values computed from the correlation equations. The results show the CFD pressure drop calculations to be on the order of 20-30% lower than those obtained using the correlation equations. The CFD heat transfer values are on the order of $\pm 20\%$ for the finned tube cases and $+40\%$ for the plain tube cases, with respect to those given by the correlation equations. In all cases the correlation equations include adjustments for the relatively small number of tube rows in this bundle. However, in the case of the heat transfer calculation for the finned tubes from [3] this adjustment is rather rough (factor of $\frac{1}{2}$ on the first tube and $\frac{3}{4}$ on the second tube, as compared with tubes deeper in the bundle).

The level of agreement obtained between the CFD pressure drop results and the correlation equations is acceptable. As described below, further mesh refinement would improve the agreement by approximately 12%. The agreement between the correlation equations and the underlying data is not known but deviations on the order of the deviation between the CFD results and those from the correlation equations are typical of the point-to-point agreement between these equations and data.

The level of agreement between the CFD heat transfer results and the correlation equations is acceptable for the finned tube cases. In fact, the two correlations considered bracket the CFD results. The agreement is not as good for the plain tube cases. This may be due to a combination of turbulence modeling issues and mesh refinement (see below). Since the major interest of this work is in the simulation of finned tubes, the results obtained here are encouraging.

Table 4
Comparison of CFD Results with Correlation Equations

| Eu Ratio (CFD/Correlation) [2] | | Nu Ratio | | | |
|-----------------------------------|----------|-----------------------|----------|-----------------------|----------|
| | | (CFD/Correlation) [3] | | (CFD/Correlation) [4] | |
| w/ fins | w/o fins | w/ fins | w/o fins | w/ fins | w/o fins |
| 0.73 | 0.80 | 1.27 | 1.45 | 0.87 | 1.38 |
| 0.83 | 0.89 | 1.46 | 1.57 | 1.00 | 1.51 |
| 0.64 | 0.81 | 1.06 | 1.34 | 0.72 | 1.29 |
| 0.71 | 0.85 | 1.29 | 1.40 | 0.88 | 1.35 |
| 0.75 | 0.74 | 1.25 | 1.48 | 0.85 | 1.40 |
| 0.73 | - | 1.36 | - | 0.89 | - |
| 0.73 | - | 1.18 | - | 0.83 | - |
| 0.74 | - | 1.17 | - | 0.82 | - |
| 0.73 | - | 1.32 | - | 0.88 | - |
| 0.70 | - | 1.21 | - | 0.82 | - |
| 0.76 | - | 1.31 | - | 0.89 | - |

Sensitivity Studies

Mesh Sensitivity

The sensitivity of the solution to mesh refinement was tested by constructing a 2D version of the plain tube version of Case 1. The mesh was refined until the computed pressure drop stabilized. The results are shown in Table 5. The pressure drop stabilizes when the mesh size is dropped from 1 mm to 0.75 mm. Further decrease to 0.5 mm has only minor effect. The results with a 1 mm mesh are 9% below the stabilized value. The results for the 3D model with a 1 mm mesh are 12% below the stabilized value. This difference between the 2D and 3D models is most likely due the fact that while the mesh is nominally 1 mm in the 3D model, the actual mesh ranges from 0.5 mm to 2 mm. Based on these results we can conclude that the solutions reported herein are nearly, but not completely, mesh independent. Since element count scales with the cube of mesh size, it is expected that the 3D model would need approximately 4.8 million elements to achieve complete mesh independence.

Table 5
Mesh Refinement Study Results

| Mesh Size | Pressure Drop over 6 Plain Tubes (Case 1) | |
|-----------|---|----------|
| | 2D Model | 3D Model |
| 2 mm | 184.7 Pa | - |
| 1 mm | 218.3 Pa | 209.8 |
| 0.75 mm | 241.5 Pa | - |
| 0.5 mm | 239.7 Pa | - |

Turbulence Modeling

Due to the separated wakes that occur in flow through a tube bundle, it is expected that the details of turbulence modeling will be important to the accuracy of the results. All of the solutions reported herein have been obtained using the standard k- ϵ model. This is the default model for most industrial problems. While this model is not preferred for calculation of flow over a single plain tube at low Reynolds numbers, the constraint imposed by adjacent tubes and fins makes this model an acceptable first choice for analyzing finned tube bundles. Work with other turbulence models is ongoing. In particular, since FIV simulations are inherently time-dependent, use of large eddy simulation (LES) techniques will be evaluated.

Of even greater importance than the turbulence model selected is the choice of wall functions. The standard wall functions make use of the “Law of the Wall” [5], assuming a universal shape for the boundary layer. Use of this model is valid for meshes with a near-wall spacing given by

$$30 < y^+ < 300,$$

where y^+ is the non-dimensional distance from the wall to the center of the first element adjacent to the wall. In the tube bundle models y^+ is on the order of 5, meaning that the assumption behind the use of the standard wall functions is violated. For this reason, FLUENT’s enhanced wall functions [1, pp. 12-68 – 12-71] were used in all calculations.

In order to evaluate the improvement gained by using the enhanced wall functions, Case 1-11 were run using both the standard and enhanced wall functions and the results compared. This comparison is presented in Table 6 below. This table shows the ratio of the Eu and Nu results computed with enhanced wall functions to those obtained with standard wall functions. The largest change is seen in the calculation of pressure drop for the finned tubes, where an improvement of approximately 20% is obtained using the enhanced wall functions. Since these are the configurations that we are most interested in, the benefits of using the enhanced wall functions are clear.

Table 6
Comparison of Enhanced and Standard Wall Functions

| Ratios (Enhanced/Standard) | | | |
|----------------------------|----------|----------|----------|
| Eu Ratio | | Nu Ratio | |
| w/ fins | w/o fins | w/ fins | w/o fins |
| 1.21 | 1.06 | 1.11 | 1.10 |
| 1.08 | 1.03 | 1.07 | 0.98 |
| 1.31 | 1.06 | 1.19 | 1.17 |
| 1.30 | 1.06 | 1.13 | 1.13 |
| 1.14 | 1.06 | 1.11 | 1.08 |
| 1.17 | - | 1.13 | - |
| 1.19 | - | 1.12 | - |
| 1.20 | - | 1.12 | - |
| 1.20 | - | 1.12 | - |
| 1.16 | - | 1.13 | - |
| 1.20 | - | 1.14 | - |

Conclusions

The CFD modeling of finned tube bundles shows promising results for calculation of pressure drop over the bundle and thus for drag on individual tubes. The heat transfer results agree well with correlation equations for finned tubes, though the comparison is not as good for plain tubes. Application of an alternative turbulence model may improve the plain tube heat transfer results.

The goal of using models such as these for calculation of FIV in tube bundles is obtainable. Based on the findings of the mesh refinement study, a mesh of 4.8 million elements would be required to obtain a mesh-independent solution to a 3D model of a single column of six tubes. This could be reduced to 4 million elements by shortening the approach mesh without impairing the accuracy of the simulation. Judicious grading of the mesh could reduce this total further, perhaps to 3.5 million elements. Using this number, for an FIV model encompassing 6 tube rows and 6 columns, the minimum size needed to simulate tube motion, the total element count would be approximately 20 million. This would be a large model that would need to be solved for transient flow. However, given a moderately sized computing cluster, on the order of 32-64 processors, solutions could be obtained over a number of days. While analysis of finned tube bundle FIV is not yet a turn-key engineering calculation, the tools for accurate 3D simulation are currently available and can be applied with the use of a sufficiently large computational cluster.

Acknowledgements

We would like to thank Harbi Pordal and Anup Paul for their advice concerning the development of the CFD models used in this work.

References

1. FLUENT 6.3 Users Manual, ANSYS, Inc., 2006.
2. Zukauskas, A. and Ulinskas, R. in Hewitt, G. F. ed., *Handbook of Heat Exchanger Design*, New York, New York: Begell House, Inc., 1992, pp. 2.2.4-1 – 2.2.4-17.
3. Gnielinski, V., Zukauskas, A. and Skrinska, A., in Hewitt, G. F. ed., *Handbook of Heat Exchanger Design*, New York, New York: Begell House, Inc., 1992, pp. 2.5.3-1 – 2.5.3-16.
4. Hewitt, G. F., Shires, G. L., and Bott, T. R., *Process Heat Transfer*, Boca Raton, Florida: CRC Press, Inc., 1994, pp.73 – 88.
5. Hinze, J. O., *Turbulence*, 2nd ed., New York, New York: McGraw-Hill, 1975, pp. 586-770.